

## Supporting information for: “Si<sub>1-x</sub>Ge<sub>x</sub> nanoantennas with tailored Raman response and light-to-heat conversion for advanced sensing applications”

E. Mitsai,<sup>1</sup> M. Aouassa,<sup>2</sup> L. Hassayoun,<sup>2</sup> D. Storozhenko,<sup>1</sup> A. Mironenko,<sup>3</sup>  
S. Bratskaya,<sup>3,4</sup> S. Juodkazis,<sup>5,6</sup> S. Makarov,<sup>7</sup> and A. Kuchmizhak<sup>1,4,\*</sup>

<sup>1</sup>*Institute of Automation and Control Processes, Far Eastern Branch,  
Russian Academy of Sciences, Vladivostok 690041, Russia*

<sup>2</sup>*Laboratory of Micro-Opto-electronic and Nanostructures (LMON),  
Department of Physics, Faculty of Sciences, 5019 Monastir, Tunisia*

<sup>3</sup>*Institute of Chemistry, Far Eastern Branch, Russian Academy of Sciences, Vladivostok 690022, Russia*

<sup>4</sup>*Far Eastern Federal University, Vladivostok 690090, Russia*

<sup>5</sup>*Swinburne University of Technology, John st., Hawthorn 3122, Victoria, Australia*

<sup>6</sup>*Melbourne Centre for Nanofabrication, ANFF, 151 Wellington Road, Clayton, VIC 3168, Australia*

<sup>7</sup>*ITMO University, 197101 St. Petersburg, Russia*

Active light-emitting all-dielectric nanoantennas recently have demonstrated a great potential to be highly efficient nanoscale light sources owing to their strong luminescent and Raman responses. However, their large-scale fabrication faces a number of problems related to productivity limits of existing lithography techniques. Thus, high-throughput fabrication strategies allowing also in a simple way to tailor of the nanoantennas emission and thermal properties in the process of their fabrication are highly desirable for various application. Here, we propose a cost-effective approach to large-scale fabrication of Si<sub>1-x</sub>Ge<sub>x</sub> alloyed Mie nanoresonators possessing enhanced Raman response which can be simply tailored via tuning the Ge concentration. Moreover, Ge content also allows for the gradual change of complex refractive index of the produced Si<sub>1-x</sub>Ge<sub>x</sub> alloy, which affects the ratio between radiative and nonradiative losses in Si<sub>1-x</sub>Ge<sub>x</sub> nanoantennas, being crucial for optimization of their optical heating efficiency. Composition-tunable Si<sub>1-x</sub>Ge<sub>x</sub> nanoantennas with optimized size, light-to-heat conversion and Raman response are implemented for non-invasive sensing of 4-aminothiophenol molecules with a temperature feedback modality and high subwavelength spatial resolution. The results are important for an advanced multichannel optical sensing, providing an information on analyte's composition, analyte-nanoantenna temperature response and spatial position.

---

\* Corresponding Author; [alex.iacp.dvo@mail.ru](mailto:alex.iacp.dvo@mail.ru)

# S1. RAMAN MAPPING OF THE GE CONCENTRATION IN THE DIFFERENT SAMPLE AREAS

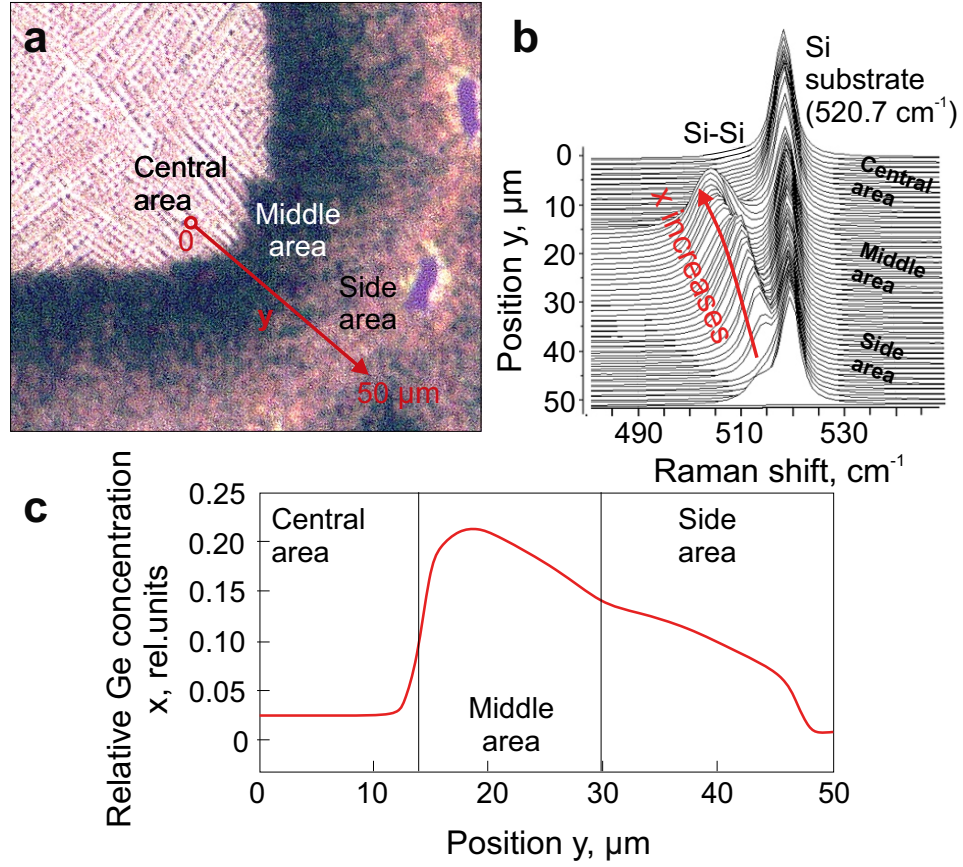


Figure S1. (a) Optical image of some representative sample area used to analyze relative Ge composition  $x$  as a function of the distance  $y$  from the central area. Three characteristic areas are indicated on the image. (b) Series of Raman spectra measured along the red line marked in (a). (c) Relative Ge composition  $x$  as a function of position from the central area  $y$ . The actual Ge composition in the alloyed nanoparticles is recalculated from the Raman spectra using the well-known expression for strain-relaxed alloys  $x = (520.7 - \omega_{Si-Si})/68$ .

## S2. DISPERSION CURVES FOR SILICON AND GERMANIUM

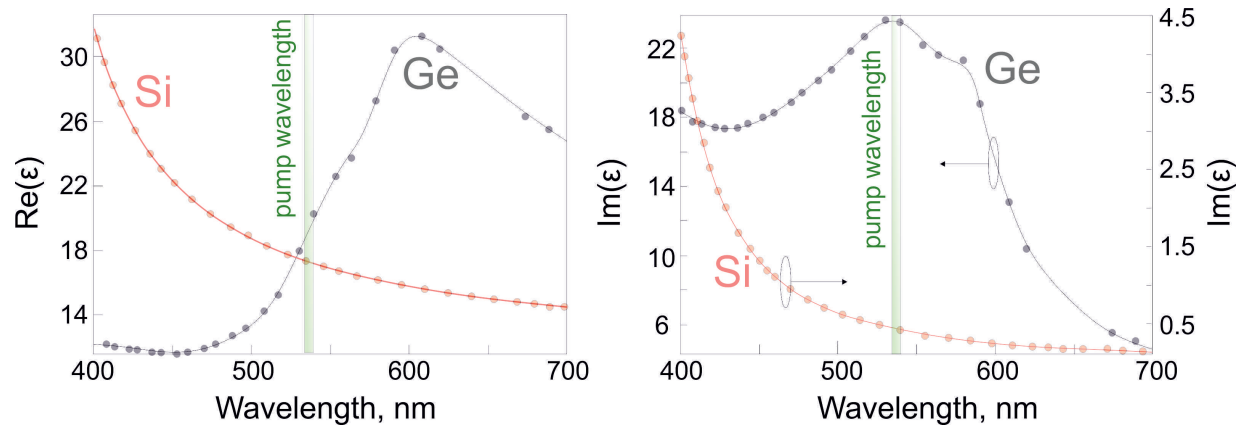


Figure S2. Real and imaginary parts of dielectric permittivity of Si and Ge in the visible spectral range. The Raman pump wavelength is marked by green.

### S3. FIELD ENHANCEMENT IN THE GAP BETWEEN TWO NANOPARTICLES

Here, we provide the numerical calculations results showing the pronounced E-field enhancement in the gap area between two identical  $\text{Si}_{0.93}\text{Ge}_{0.07}$  nanoparticles both having base diameter of 220 nm. In general, the enhancement factor in such system depends strongly on the gap size rather than on the dimensions of the nanoparticles and can reach  $E_{out}^4/E_0^4 \approx 10^5$  for nanoscale gaps.

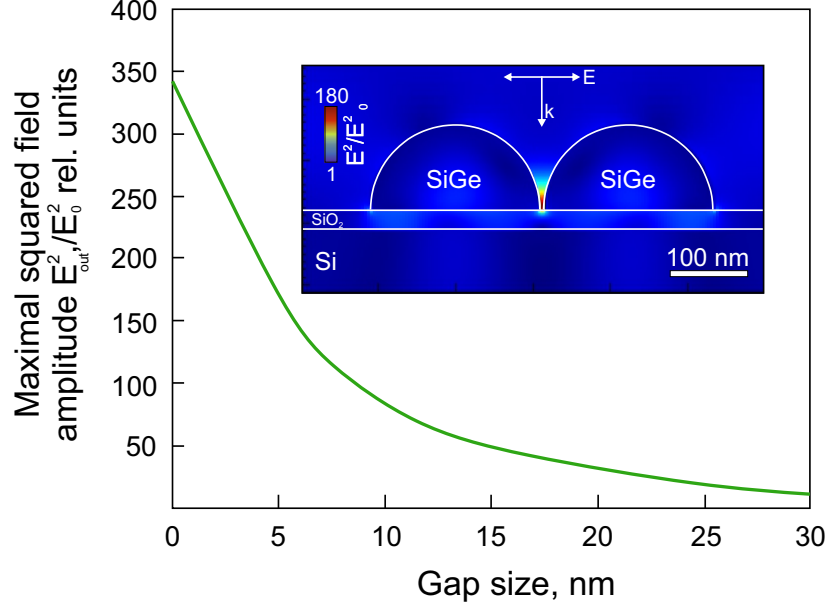


Figure S3. Calculated maximal normalized squared electric field amplitude  $E^2/E_0^2$  as a function of gap size between two identical  $\text{Si}_{0.93}\text{Ge}_{0.07}$  nanoparticles both having base diameter of 220 nm. Inset shows the calculated 2D map of the squared electric field amplitude  $E$  in the gap area of two identical  $\text{Si}_{0.93}\text{Ge}_{0.07}$  nanoparticles. The gap size is 5 nm.

#### S4. TEMPERATURE-INDUCED SHIFT OF THE SI-SI RAMAN MODE OF $\text{Si}_{1-x}\text{Ge}_x$ NANOPARTICLES

Shift of the spectral maximum of the c-Si phonon mode of pure silicon can be converted into the corresponding temperature shift  $\Delta T$  via the well-known expression [1]:

$$\Omega(T) = \Omega_0 + A \left( 1 + \frac{2}{e^x - 1} \right) + B \left( 1 + \frac{3}{e^y - 1} + \frac{3}{(e^y - 1)^2} \right), \quad (\text{S1})$$

where  $\Omega_0 = 528 \text{ cm}^{-1}$ ,  $A = -2.96 \text{ cm}^{-1}$ ,  $B = -0.174 \text{ cm}^{-1}$ ,  $x = \hbar\Omega_0/2kT$ , and  $y = \hbar\Omega_0/3kT$  for crystalline silicon.

Taking into account that for Si-rich  $\text{Si}_{1-x}\text{Ge}_x$  alloys, (at  $x < 0.3$ ) the relative spectral shift of the Si-Si Raman mode demonstrates almost similar  $\Delta(T)$  dependence being compared to pure c-Si [2], the calculated data from Fig. S4 can be well applicable to access the actual temperature of the alloyed nanoparticles discussed in this paper.

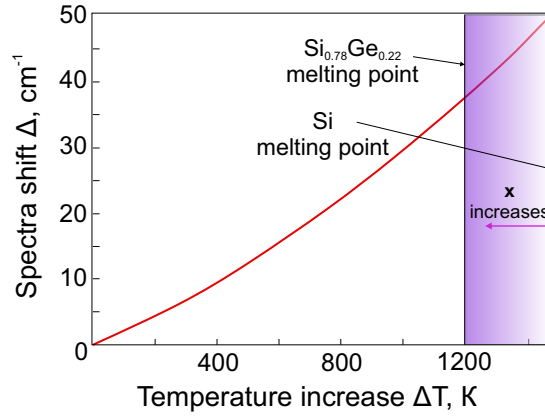


Figure S4. Dependence of Raman shift  $\Delta$  on temperature increase  $\Delta T$  for bulk  $\text{Si}_{0.78}\text{Ge}_{0.22}$  alloy film calculated according to [2]. The corresponding decrease of the melting temperature of the alloyed caused by increase of the relative Ge composition  $x$  is shown as a purple area. The melting points for pure Si film and  $\text{Si}_{0.78}\text{Ge}_{0.22}$  alloy are also indicated.

### S5. LASER-INDUCED IRREVERSIBLE MODIFICATION OF ALLOYED NANOPARTICLES

Here, the side-view SEM images of the isolated  $\text{Si}_{0.78}\text{Ge}_{0.22}$  alloyed nanoparticles having approximately similar diameter  $\approx 250$  nm irradiated by laser spot of Raman microscope at variable pump intensity. For all particles, the irradiation time was 5 sec. According to the data from Fig. 3c, at such relatively high Ge concentration  $x$ , owing to efficient light-to-heat conversion the alloyed nanoparticles reach the irreversible modification via melting ( $T_{\text{melt}} \approx 1450$  K) at pump intensity of  $I=28 \text{ mW}/\mu\text{m}^2$ , which is clearly observed in Fig. S5(b). Further increase of the pump intensity results in substantial reshaping of the nanoparticle – from partial removal of the molten material from its central part to complete destruction at  $I=65 \text{ mW}/\mu\text{m}^2$ . Noteworthy, for alloyed nanoparticles with low Ge composition, we did not find the thermally damaged nanoparticles even at  $I=65 \text{ mW}/\mu\text{m}^2$  pump intensity owing to their less efficient laser heating and increased melting temperature  $T_{\text{melt}} \approx 1640$  K.

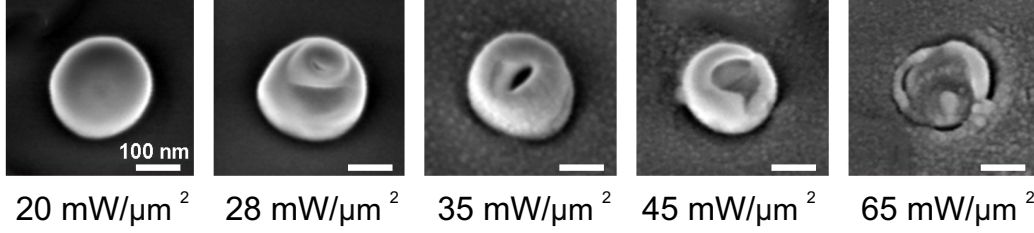


Figure S5. Series of side-view (view angle of  $40^\circ$ ) SEM images of laser-heated  $\text{Si}_{0.78}\text{Ge}_{0.22}$  nanoparticles irradiated at increased incident intensity for 5 sec.

## S6. THERMOGRAVIMETRIC ANALYSIS

Thermogravimetry studies were carried out using a Q-1500 derivatograph in an open platinum crucible (100 mg sample) at a heating rate of  $1.25^{\circ}/\text{min}$ . Figure S6 shows the results obtained for 4-ATP analyte molecules used in this study. The results provide the critical temperature of  $160^{\circ}\text{C}$  for the measured analyte molecules.

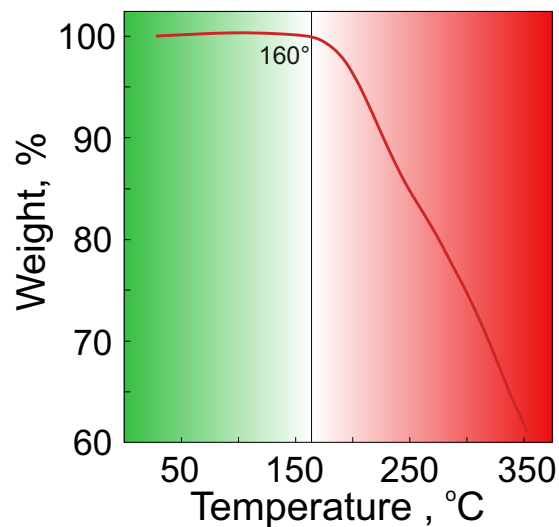


Figure S6. Thermogravimetric curve of the 4-ATP analyte.

- 
- [1] M. Balkanski, R. Wallis, and E. Haro, Phys. Rev. B **28**, 1928 (1983).
  - [2] H. Burke and I. Herman, Phys. Rev. B **48**, 15016 (1993).